Medical and Research Publications
International Open Access

Research Article **Journal of MAR Neurology and Psychology (Volume 5 Issue 6)**

Mri-Flair Intraventricular CSF Pulsation Artifacts (VCSFA) in UWS Patients

Jesús Perez-Nellar[1], Calixto Machado*[2], Rafael Rodríguez[3], Yanin Machado[2], Mauricio Chinchilla [2], Arthur Schiff [4], Beata Drobná Sániová [5], Michal Drobný [5]

1. Hermanos Ameijeiras Hospital, Stroke Unit, Havana, Cuba.

2. Institute of Neurology and Neurosurgery, Department of Clinical Neurophysiology, Havana, Cuba

3. International Center for Neurological Restoration, Havana, Cuba

4. Emory University School of Medicine, 201 Dowman Dr, Atlanta, GA 30322

5. Comenius University in Bratislava, Slovak Republic

Corresponding Author: Calixto Machado, MD, Ph.D., FAAN, President, Cuban Society of Clinical Neurophysiology, Instituto de Neurología y Neurocirugía, 29 y D, Vedado, Apartado Postal 4268, La Habana 10400.

Received Date: November 16, 2022

Published Date: December 01, 2022

Abstract

One of the major limitations of FLAIR imaging is the ventricular CSF pulsation artifact (VCSFA). This artifact could compromise the study of ventricular abnormalities by leading to false-negative or false-positive interpretations. We report four young unresponsive wakefulness syndrome (UWS) patients with severe ventriculomegaly and brain atrophy who showed VCSFA on MR imaging. FLAIR axial images showed the presence of a hyperintensity occupying the third, fourth lateral ventricles and the aqueduct of Sylvius. VCSFA was more prominent in the third and fourth ventricles compared with the lateral ventricles. In PVS, both severe ventriculomegaly and brain atrophy might induce non-appropriate CSF circulation nulling, which remains hyperintense on axial FLAIR images, leading to VCSFA coming out. This is the first report in the literature about the presence of VCSFA in UWS patients.

Keyword: *MRI; FLAIR; ventricular CSF pulsation artifact (VCSFA); unresponsive wakefulness syndrome (UWS); cerebrospinal fluid; ventricles.*

Introduction

The fast fluid-attenuated inversion recovery (FLAIR) magnetic resonance imaging (MRI) technique was first reported by Hajnal et al.**[**1, 2**]** Normal cerebral spinal fluid (CSF) has long T1 and long T2 times manifest as dark signals on T1-weighted images and bright signals on T2-weighted images. FLAIR imaging results in nulling and dark CSF signals. The ability to perform FLAIR imaging with fast spin-echo (FSE) sequences time nulls the CSF signal, providing heavy T2 weighting due to its very long echo time. **[**3-9**]**

The superiority of FLAIR imaging compared with T1- and T2-weighted Imaging has been suggested in evaluating various disorders, such as stroke, multiple sclerosis, infections, hypertensive encephalopathy, and cerebral hemorrhage. **[**4, 5, 9-21**]**

Nonetheless, one of the major limitations of FLAIR imaging is ventricular CSF pulsation artifact (VCSFA). This artifact could compromise the sensitivity and specificity of FLAIR images by leading to false-negative or false-positive interpretations of ventricular abnormalities. **[**22-25**]**

We report four young unresponsive wakefulness syndrome (UWS) patients with marked ventriculomegaly and brain atrophy who showed the VCSFA on FLAIR MRI. This is the first report in the literature about the presence of VCSFA in UWS patients.

Methods

We studied four patients (ranging from 12 to 31 years old) who suffered hypoxic-ischemic insult resulting in UWS of long-term clinical evolution (4-8 years). The patients fulfilled current diagnostic criteria for UWS 26-36: no evidence of awareness of self or environment, no interaction with others, and no comprehension or expression of language. Noxious stimuli frequently resulted in massive stretching or startle reactions without habituation, sometimes with massive flexor responses. They were occasionally grimacing following stimulation. Nonetheless, external stimuli did not evoke purposefully, sustained, and reproducible voluntary behavioral responses. Patients were assessed by the Coma Recovery Scale Revisited (CRS-R).27, 37-39 Patients' demographic features are summarized in table 1.

PVS patients	OC	JM	RH	AG
Age	12	18	18	31
Sex	male	male	male	male
Skin color	mestee	black	mestee	black
Etiology	Near drown	Near drown	Near drown	Anesthetic accident
PVS duration	6 years	8 years	4 years	6 years
CRS-R scale	6 points	4 points	3 points	4 points

CRS-R: Coma Recovery Scale Revisited

Table 1. Patients' Demographic features.

Patients were studied by a 1.5T MR scanner (Symphony, Siemens). FLAIR technique description is found elsewhere.40 Two independent observers reviewed MRI studies to detect the VCSFA in the aqueduct of Sylvius and the lateral, third, and fourth ventricles. VCSFA intensity was classified as slight, moderate, and high by the two independent observers.

The Institute of Neurology and Neurosurgery IRB, Havana, Cuba, approved this study.

Results

The VCSFA was found in all patients and was more prominent in the third and fourth ventricles than the lateral ventricles (Table 2).

PVS patients	OC	JM	RH	AG
Lateral ventricles	+	+	+	+
III ventricle	+++	+++	++	+++
Aqueduct	++	+++	+	+
IV ventricle	+++	++	++	++

\+ Slight VCSFA intensity

++ Moderate VCSFA intensity

+++ High VCSFA intensity

Table 2. VCSFA intensity in cerebral ventricles and aqueduct of Sylvius.

Figure 1 presents MRI data sets on axial views from patient OC (A to F images). MRI FLAIR axial images showed the VCSFA in the fourth and third ventricles; meanwhile, this artifact was comparatively less pronounced in the lateral ventricles, visualized as small white spots. There was also parenchymal atrophy and white matter hyperintensity. MR T1 axial images of the same patient (D to F) revealed severe brain atrophy in both cerebral hemispheres, associated with dilated ventricles and wide cerebral sulci, but no intraventricular abnormalities were found. The VCSFA was found on axial images in one patient but was not detected on sagittal planes.

Figure 2. shows the FLAIR axial image of patient AG demonstrating fourth and third ventricular CSF pulsation artifacts (arrows). There is severe parenchymal atrophy.

Figure 3 presents the FLAIR axial image of patient JM, demonstrating a huge atrophy with ventriculomegaly. A severe ventricular CSF pulsation artifact (arrows) is visualized in the fourth ventricle (A-B), aqueduct (C), and third ventricle (D-E).

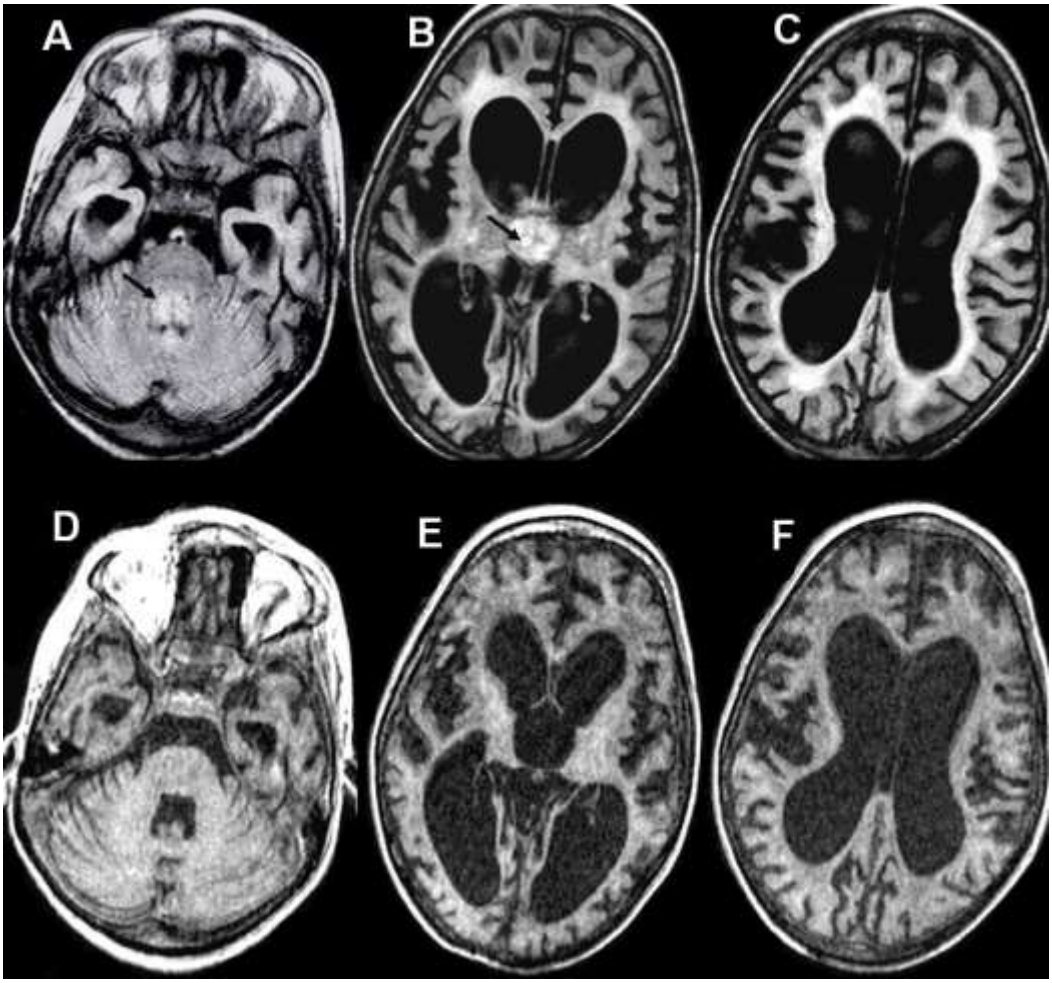

Figure 1. Brain MRI of patient OC. FLAIR axial images show the presence of a prominent hyperintensity (arrows) occupying the fourth (A) and third (B) ventricles. MRI-T1 images in axial planes reveal marked atrophy in both cerebral hemispheres, associated with dilated ventricles and wide cerebral sulci, but no intraventricular abnormalities were found (C and D). In one case, severe VCSFA is present on axial images but disappears on sagittal planes (F).

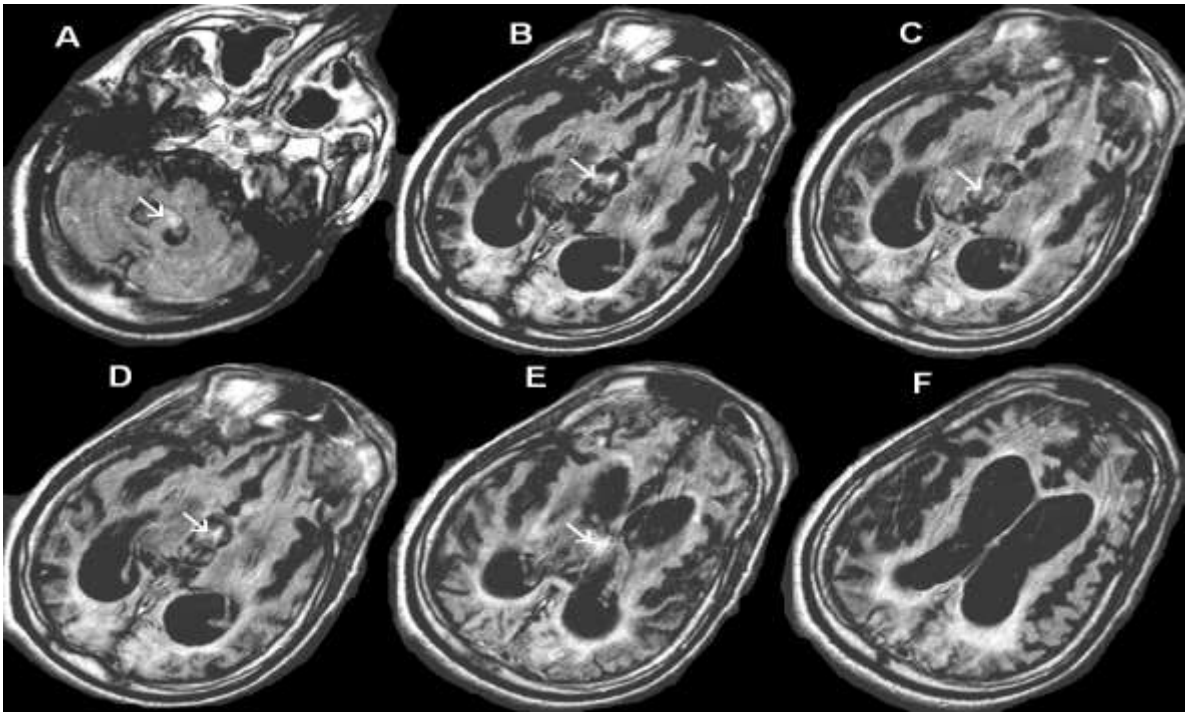

Figure 2. FLAIR axial image (patient AG) with fourth and third ventricular CSF pulsation artifact (arrows). There is severe parenchymal atrophy.

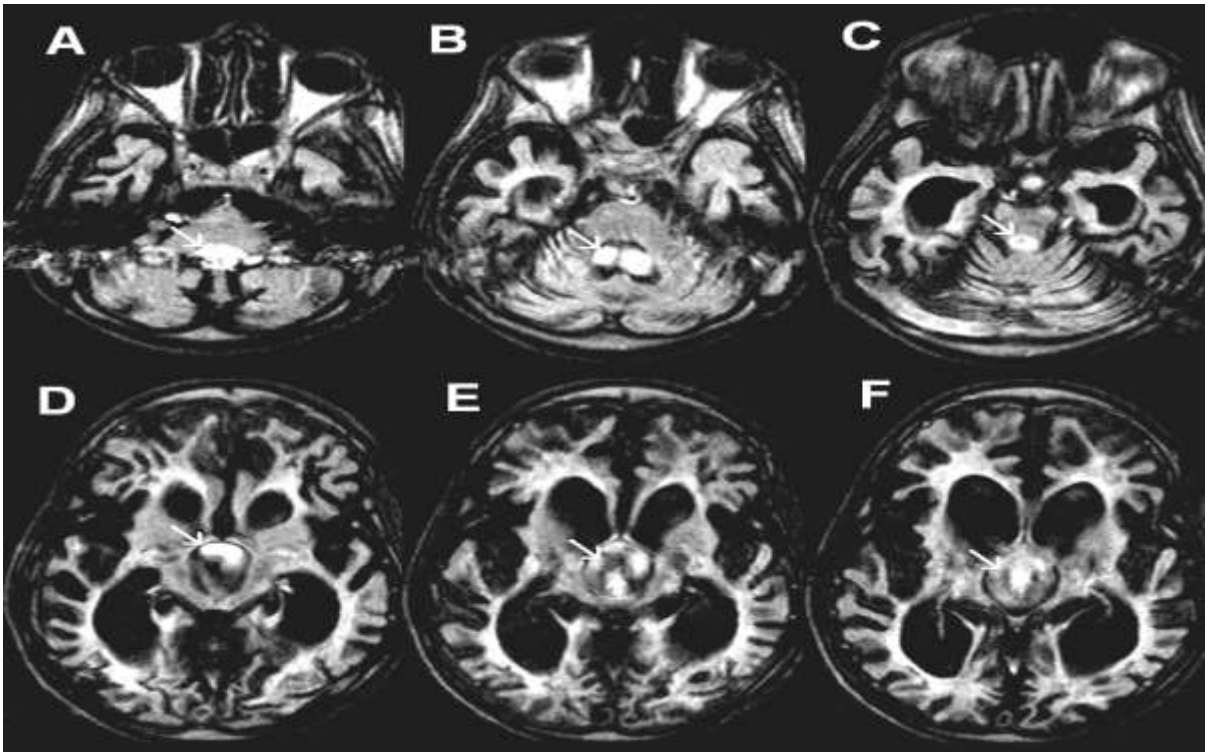

Figure 3. FLAIR axial image (patient JM). There is severe atrophy with ventriculomegaly. A severe ventricular CSF pulsation artifact (arrows) is visualized in the fourth ventricle (A-B), aqueduct (C), and third ventricle (D-E).

Discussion

The prominent hyperintensity occupying the cerebral ventricles in our patients most probably represents the VCSFA due to an inversion delay and ghosting effects. VCSFA might obscure or mimic intraventricular lesions, especially in the third and fourth ventricles. **[**1, 2, 23, 41-52**]**

The most important contributor to VCSFA is an inflow of non-nulled cerebral spinal fluid (CSF) from the superior or inferior areas. When CSF goes into the brain sections between the inversion pulse and the commencement of signal sampling, it is not appropriately nulled and remains hyperintense on axial FLAIR images. Hence, the causes of VCSFA seem to be multifactorial. **[**1, 2, 23, 43-49, 53-56**]**

This is analogous to the signal produced by the inflow of fresh blood on time-of-flight MR angiograms, and only instead of saturation effects, the VCSFA is due to the effects of inversion delay.**[**23, 57-60**]** CSF enters the brain sections between the inversion pulse and the beginning of signal sampling; hence, it is not correctly nulled and remains hyperintense on axial FLAIR images. **[**6, 19, 22, 23, 41, 46, 47, 61-63**]**

The increased severity and frequency of VCSFA in the third and fourth ventricles are most likely multifactorial. One likely cause is the reflux of spinal CSF into these inferior ventricles through the posterior fossa. A second factor is the increased velocity of CSF flow through the third and fourth ventricles, increasing the rate of superior entry of CSF from the lateral ventricles during the inversion delay. Ghost pulsation effects also appear to contribute to VCSFA. Because CSF is moving in the ventricles, any residual non-nulled CSF will cause pulsation artifacts in many places. One manifestation of this ghosting is the placement of redundant CSF signals across the phase-encoding axis in a manner that could obscure or mimic brain parenchymal lesions. Inflow and ghost pulsation effects are artifacts caused by flow and are thus related. The difference is that optimal gradient moment nulling (e.g., accounting for velocity, acceleration, jerk, etc.) might reduce the effect of ghosting but would not affect the inversion delay artifact. Conversely, wider inversion pulses might help reduce the signal from inflowing CSF, but any moving protons will still cause ghosting of whatever signal they contribute. **[**11, 23, 46, 47, 64-68**]**

Bakshi et al. reported that increasing ventricular size and, to a lesser extent, increasing age were significantly associated with VCSFA. **[**23**]** In UWS cases is frequent to find marked brain atrophy and ventriculomegaly. These morphological features put forth their maximal force on the CSF circulation. Ventriculomegaly may induce an increment of CSF flow velocity through the third and fourth ventricles. **[**34, 35, 69, 70**]**

Another possible mechanism could be the reflux of spinal CSF into the fourth and third ventricles from the cisterna magna. Some authors have shown increased passage of subarachnoid dye into the fourth ventricle from the cisterna magna in cases of ventriculomegaly due to brain volume loss, as occurs in hydrocephalus. **[**71-73**]** This reflux may also be enhanced in normal-pressure and pyogenic meningitis.**[**74-76**]**

Brain atrophy might produce a decrement in the compliance of periventricular tissues that may allow for the more vigorous transmission of systolic and diastolic pulsations to the ventricles, further increasing CSF velocity. These strong CSF pulsations that occur in synchrony with the systole and diastole set forth their maximal force at the base of the brain through the third ventricle, where CSF velocities are also maximal. Hence, marked ventriculomegaly and brain atrophy might explain the presence of the VCSFA in UWS cases because CSF circulation might not be appropriately nulled, remaining hyperintense on MR axial images. **[**23, 72, 74, 77-79**]**

In one case, the VCSFA was found on axial images, but it was not detected on sagittal planes. This is likely because sagittal Imaging induces the required nulling of in-plane midline brain and cervical spinal CSF before the fluid arrives at the third and fourth ventricles during readout. (i.e., CSF flow remains in-plane, and no inflow of non-nulled CSF occurs). **[**23, 80**]**

Several authors have proposed technical variations to reduce this artifact, such as using a wider slice-selective inversion to increase the inversion of CSF outside the imaging section or using other section-selective inversion pulses to utilize cardiac synchronization during MRI acquisition.**[**81-83**]** Other authors have recommended using a non-slice-selective inversion pulse to eliminate the VCSFA using the K-space reordered by Inversion-time for each Slice Position (KRISP) technique in order to achieve constant contrast in a multislice acquisition.**[**46, 47**]**

We conclude that it is extremely important to consider the possible presence of VCSFA in UWS patients because it may induce false-negative or false-positive diagnoses of intraventricular abnormalities.

References

1. Hajnal JV, Collins AG, White SJ, et al. Imaging of human brain activity at 0.15 T using fluid attenuated inversion recovery (FLAIR) pulse sequences. Magn Reson Med 1993 ;30:650-653.

2. Hajnal JV, Bryant DJ, Kasuboski L, et al. Use of fluid attenuated inversion recovery (FLAIR) pulse sequences in MRI of the brain. J Comput Assist Tomogr 1992;16:841-844.

3. Eliezer M, Vaussy A, Toupin S, et al. Iterative denoising accelerated 3D SPACE FLAIR sequence for brain MR imaging at 3T. Diagn Interv Imaging 2021.

4. Hannoun S, Heidelberg D, Hourani R, et al. Diagnostic value of 3DFLAIR in clinical practice for the detection of infratentorial lesions in multiple sclerosis in regard to dual echo T2 sequences. Eur J Radiol 2018;102:146-151.

5. Schmidt P, Gaser C, Arsic M, et al. An automated tool for detection of FLAIR-hyperintense white-matter lesions in Multiple Sclerosis. Neuroimage 2012;59:3774-3783.

6. von Kalle T, Blank B, Fabig-Moritz C, et al. Reduced artefacts and improved assessment of hyperintense brain lesions with BLADE MR imaging in patients with neurofibromatosis type 1. Pediatr Radiol 2009;39:1216-1222.

7. Bonhomme GR, Waldman AT, Balcer LJ, et al. Pediatric optic neuritis: brain MRI abnormalities and risk of multiple sclerosis. Neurology 2009;72:881-885.

8. Wijdicks EF, Campeau NG, Miller GM. MR imaging in comatose survivors of cardiac resuscitation. AJNR Am J Neuroradiol 2001;22:1561-1565.

9. Stevenson VL, Parker GJ, Barker GJ, et al. Variations in T1 and T2 relaxation times of normal appearing white matter and lesions in multiple sclerosis. J Neurol Sci 2000;178:81-87.

10. Kirschen MP, Licht DJ, Faerber J, et al. Association of MRI Brain Injury With Outcome After Pediatric Out-of-Hospital Cardiac Arrest. Neurology 2021;96:e719-e731.

11. Sharma R, Sekhon S, Cascella M. White Matter Lesions. StatPearls. Treasure Island (FL)2021.

12. Igwe KC, Lao PJ, Vorburger RS, et al. Automatic quantification of white matter hyperintensities on T2-weighted fluid attenuated inversion recovery magnetic resonance imaging. Magn Reson Imaging 2021;85:71-79.

13. Perez-Vela JL, Ramos-Gonzalez A, Lopez-Almodovar LF, et al. **[**Neurologic complications in the immediate postoperative period after cardiac surgery. Role of brain magnetic resonance imaging**]**. Rev Esp Cardiol 2005;58:1014-1021.

14. Steen RG, Emudianughe T, Hankins GM, et al. Brain imaging findings in pediatric patients with sickle cell disease. Radiology 2003;228:216-225.

15. Lecler A, El Sanharawi I, El Methni J, Gout O, Koskas P, Savatovsky J. Improving Detection of Multiple Sclerosis Lesions in the Posterior Fossa Using an Optimized 3D-FLAIR Sequence at 3T. AJNR Am J Neuroradiol 2019;40:1170-1176.

16. Eichinger P, Schon S, Pongratz V, et al. Accuracy of Unenhanced MRI in the Detection of New Brain Lesions in Multiple Sclerosis. Radiology 2019;291:429-435.

17. Dyachenko PA, Smiianova OI, Dyachenko AG. Meningo-Encephalitis in a Middle-Aged Woman Hospitalized for Covid-19. Wiad Lek 2021;74:1274-1276.

18. Varadan B, Shankar A, Rajakumar A, et al. Acute hemorrhagic leukoencephalitis in a COVID-19 patient-a case report with literature review. Neuroradiology 2021;63:653-661.

19. Wu H, Yu H, Joseph J, Jaiswal S, Pasham SR, Sriwastava S. Neuroimaging and CSF Findings in Patients with Autoimmune Encephalitis: A Report of Eight Cases in a Single Academic Center. Neurol Int 2022;14:176-185.

20. Weston P, Behr S, Garosi L, Maeso C, Carrera I. Ischemic stroke can have a T1w hyperintense appearance in absence of intralesional hemorrhage. Front Vet Sci 2022;9:932185.

21. Thomas MF, Kofler F, Grundl L, et al. Improving Automated Glioma Segmentation in Routine Clinical Use Through Artificial Intelligence-Based Replacement of Missing Sequences With Synthetic Magnetic Resonance Imaging Scans. Invest Radiol 2022;57:187-193.

22. Ogbole GI, Soneye MA, Okorie CN, Sammet S. Intraventricular cerebrospinal fluid pulsation artifacts on low-field magnetic resonance imaging: Potential pitfall in diagnosis? Niger Med J 2016;57:59-63.

23. Bakshi R, Caruthers SD, Janardhan V, Wasay M. Intraventricular CSF pulsation artifact on fast fluid-attenuated inversion-recovery MR images: analysis of 100 consecutive normal studies. AJNR Am J Neuroradiol 2000;21:503-508.

24. Jeong HK, Oh SW, Kim J, Lee SK, Ahn SJ. Reduction of Oxygen-Induced CSF Hyperintensity on FLAIR MR Images in Sedated Children: Usefulness of Magnetization-Prepared FLAIR Imaging. AJNR Am J Neuroradiol 2016;37:1549-1555.

25. Krupa K, Bekiesinska-Figatowska M. Artifacts in magnetic resonance imaging. Pol J Radiol 2015;80:93-106.

26. Annen J, Filippini MM, Bonin E, et al. Diagnostic accuracy of the CRS-R index in patients with disorders of consciousness. Brain Inj 2019;33:1409-1412.

27. Formisano R, Contrada M, Iosa M, Ferri G, Schiattone S, Aloisi M. Coma Recovery Scale-Revised With and Without the Emotional Stimulation of Caregivers. Can J Neurol Sci 2019;46:607-609.

28. Lesenfants D, Habbal D, Chatelle C, Soddu A, Laureys S, Noirhomme Q. Toward an Attention-Based Diagnostic Tool for Patients With Locked-in Syndrome. Clin EEG Neurosci 2018;49:122-135.

29. Vanhaudenhuyse A, Charland-Verville V, Thibaut A, et al. Conscious While Being Considered in an Unresponsive Wakefulness Syndrome for 20 Years. Front Neurol 2018;9:671.

30. Iazeva EG, Legostaeva LA, Zimin AA, et al. A Russian validation study of the Coma Recovery Scale-Revised (CRS-R). Brain Inj 2018:1-8.

31. Machado C, Rodriguez-Rojas R, Leisman G. Partial recovery of vegetative state after a massive ischaemic stroke in a child with sickle cell anaemia. BMJ Case Rep 2020;13.

32. Machado C, Estevez M, Rodriguez-Rojas R. Zolpidem efficacy and safety in disorders of consciousness. Brain Inj 2018;32:530-531.

33. Del Giudice R, Blume C, Wislowska M, et al. Can self-relevant stimuli help assessing patients with disorders of consciousness? Conscious Cogn 2016;44:51-60.

34. Machado C, Estevez M, Rodriguez R, et al. Zolpidem arousing effect in persistent vegetative state patients: autonomic, EEG and behavioral assessment. Curr Pharm Des 2014;20:4185-4202.

35. Machado C, Estevez M, Carrick FR, et al. Vegetative state is a pejorative term. NeuroRehabilitation 2012;31:345-347.

36. Machado C, Estevez M, Rodriguez R, et al. A Cuban perspective on management of persistent vegetative state. MEDICC Rev 2012;14:44-48.

37. Chaturvedi J, Mudgal SK, Venkataram T, et al. Coma recovery scale: Key clinical tool ignored enough in disorders of consciousness. Surg Neurol Int 2021;12:93.

38. Zhang Y, Wang J, Schnakers C, et al. Validation of the Chinese version of the Coma Recovery Scale-Revised (CRS-R). Brain Inj 2019;33:529-533.

39. Giacino JT, Kalmar K, Whyte J. The JFK Coma Recovery Scale-Revised: measurement characteristics and diagnostic utility. Arch Phys Med Rehabil 2004;85:2020-2029.

40. Rodriguez-Rojas R, Machado C, Alvarez L, et al. Zolpidem induces paradoxical metabolic and vascular changes in a patient with PVS. Brain Inj 2013;27:1320-1329.

41. Tanaka N, Abe T, Kojima K, Nishimura H, Hayabuchi N. Applicability and advantages of flow artifact-insensitive fluid-attenuated inversion-recovery MR sequences for Imaging the posterior fossa. AJNR Am J Neuroradiol 2000;21:1095-1098.

42. Oatridge A, Hajnal JV, Cowan FM, Baudouin CJ, Young IR, Bydder GM. MRI diffusion-weighted Imaging of the brain: contributions to image contrast from CSF signal reduction, use of a long echo time and diffusion effects. Clin Radiol 1993;47:82-90.

43. Oatridge A, Curati WL, Herlihy AH, et al. Evaluation of a FLAIR sequence designed to reduce CSF and blood flow artifacts by use of k-space reordered by inversion time at each slice position (KRISP) in high grade gliomas of the brain. J Comput Assist Tomogr 2001;25:251-256.

44. De Coene B, Hajnal JV, Gatehouse P, et al. MR of the brain using fluid-attenuated inversion recovery (FLAIR) pulse sequences. AJNR Am J Neuroradiol 1992;13:1555-1564.

45. Yapo P, Sonier CB, Franconi F, et al. **[**Use of a stimulated echo sequence in the MRI study of the brain and spine**]**. J Neuroradiol 1996;23:56-61.

46. Herlihy AH, Oatridge A, Curati WL, Puri BK, Bydder GM, Hajnal JV. FLAIR imaging using nonselective inversion pulses combined with slice excitation order cycling and k-space reordering to reduce flow artifacts. Magn Reson Med 2001;46:354-364.

47. Herlihy AH, Hajnal JV, Curati WL, et al. Reduction of CSF and blood flow artifacts on FLAIR images of the brain with k-space reordered by inversion time at each slice position (KRISP). AJNR Am J Neuroradiol 2001;22:896-904.

48. Duhamel G, de Bazelaire C, Alsop DC. Evaluation of systematic quantification errors in velocity-selective arterial spin labeling of the brain. Magn Reson Med 2003;50:145-153.

49. Andersson L, Bolling M, Wirestam R, Holtas S, Stahlberg F. Combined diffusion weighting and CSF suppression in functional MRI. NMR Biomed 2002;15:235-240.

50. Storelli L, Rocca MA, Pantano P, et al. MRI quality control for the Italian Neuroimaging Network Initiative: moving towards big data in multiple sclerosis. J Neurol 2019;266:2848-2858.

51. Wintersperger BJ, Runge VM, Biswas J, et al. Brain magnetic resonance imaging at 3 Tesla using BLADE compared with standard rectilinear data sampling. Invest Radiol 2006;41:586-592.

52. Jeong EK, Kim SE, Parker DL. High-resolution diffusion-weighted 3D MRI, using diffusion-weighted driven-equilibrium (DW-DE) and multishot segmented 3D-SSFP without navigator echoes. Magn Reson Med 2003;50:821-829.

53. Mattei C, Oevermann A, Schweizer D, et al. MRI ischemic and hemorrhagic lesions in arterial and venous territories characterize central nervous system intravascular lymphoma in dogs. Vet Radiol Ultrasound 2022.

54. O'Neill AG, Lingala SG, Pineda AR. Predicting human detection performance in magnetic resonance imaging (MRI) with total variation and wavelet sparsity regularizers. Proc SPIE Int Soc Opt Eng 2022;12035.

55. Kato Y, Naganawa S, Taoka T, Yoshida T, Sone M. Pitfalls of Using T2-contrast Enhancement Techniques in 3D-FLAIR to Detect Endolymphatic Hydrops. Magn Reson Med Sci 2022.

56. Sundermann B, Billebaut B, Bauer J, et al. Practical Aspects of novel MRI Techniques in Neuroradiology: Part 1-3D Acquisitions, Dixon Techniques and Artefact Reduction. Rofo 2022;194:1100-1108.

57. Buxton RB, Kerber CW, Frank LR. Pulsatile flow artifacts in two-dimensional time-of-flight MR angiography: initial studies in elastic models of human carotid arteries. J Magn Reson Imaging 1993;3:625-636.

58. Reddy R. Magnetic Resonance Imaging Evaluation of Perinatal Hypoxic Ischemic Encephalopathy: An Institutional Experience. J Neurosci Rural Pract 2022;13:87-94.

59. Poillon G, Horion J, Daval M, et al. MRI characteristics of intralabyrinthine schwannoma on post-contrast 4 h-delayed 3D-FLAIR Imaging. Diagn Interv Imaging 2021.

60. Vinchon M, Noule N, Tchofo PJ, Soto-Ares G, Fourier C, Dhellemmes P. Imaging of head injuries in infants: temporal correlates and forensic implications for the diagnosis of child abuse. J Neurosurg 2004;101:44-52.

61. Thomas DJ, Pennock JM, Hajnal JV, Young IR, Bydder GM, Steiner RE. Magnetic resonance imaging of spinal cord in multiple sclerosis by fluid-attenuated inversion recovery. Lancet 1993;341:593-594.

62. Kallmes DF, Hui FK, Mugler JP, 3rd. Suppression of cerebrospinal fluid and blood flow artifacts in FLAIR MR imaging with a single-slab three-dimensional pulse sequence: initial experience. Radiology 2001;221:251-255.

63. Wolf K, Luetzen N, Mast H, et al. CSF Flow and Spinal Cord Motion in Patients With Spontaneous Intracranial Hypotension: A Phase Contrast MRI Study. Neurology 2022.

64. White SJ, Hajnal JV, Young IR, Bydder GM. Use of fluid-attenuated inversion-recovery pulse sequences for Imaging the spinal cord. Magn Reson Med 1992;28:153-162.

65. Kita M, Sato M, Kawano K, et al. Online tool for calculating null points in various inversion recovery sequences. Magn Reson Imaging 2013;31:1631-1639.

66. Cianfoni A, Martin MG, Du J, et al. Artifact simulating subarachnoid and intraventricular hemorrhage on single-shot, fast spin-echo fluid-attenuated inversion recovery images caused by head movement: A trap for the unwary. AJNR Am J Neuroradiol 2006;27:843-849.

67. Mizutani K, Sumida T, Matsuda M, Ishikawa A. **[**Basic evaluation of a new technique, tailored contrast truck-fluid-attenuated driven inversion-recovery (TACT-FLADIR), to attenuate the signals of both cerebrospinal fluid and inflow artifacts**]**. Nihon Hoshasen Gijutsu Gakkai Zasshi 2004;60:1316-1324.

68. Wu HM, Yousem DM, Chung HW, Guo WY, Chang CY, Chen CY. Influence of imaging parameters on high-intensity cerebrospinal fluid artifacts in fast-FLAIR MR imaging. AJNR Am J Neuroradiol 2002;23:393-399.

69. Machado C, Estevez M, Chihchilla M, Perez-Nellar J. Disorders of Consciousness: Common Findings in Brain Injury. In: Wang KKW, ed. Neurotrauma: A Comprehensive Textbook on Traumatic Brain Injury and Spinal Cord Injury Oxford: Oxford University Press, 2018.

70. Machado C, Estevez M, Gutierrez J, et al. Recognition of the mom's voice with an emotional content in a PVS patient. Clin Neurophysiol 2011;122:1059-1060; author reply 1061-1052.

71. Zerah M, Garcia-Monaco R, Rodesch G, et al. Hydrodynamics in vein of Galen malformations. Childs Nerv Syst 1992;8:111-117; discussion 117.

72. Licata C, Cristofori L, Gambin R, Vivenza C, Turazzi S. Post-traumatic hydrocephalus. J Neurosurg Sci 2001;45:141-149.

73. Arriada N, Sotelo J. Continuous-flow shunt for treatment of hydrocephalus due to lesions of the posterior fossa. J Neurosurg 2004;101:762-766.

74. Bakshi R, Kinkel PR, Mechtler LL, Bates VE. Cerebral ventricular empyema associated with severe adult pyogenic meningitis: computed tomography findings. Clin Neurol Neurosurg 1997;99:252-255.

75. Meguins LC, Rocha AS, Laurenti MR, de Morais DF. Ventricular empyema associated with severe pyogenic meningitis in COVID-19 adult patient: Case report. Surg Neurol Int 2021;12:346.

76. Ohno N, Miyati T, Mase M, et al. Idiopathic normal-pressure hydrocephalus: temporal changes in ADC during cardiac cycle. Radiology 2011;261:560-565.

77. Tsitouras V, Sgouros S. Infantile posthemorrhagic hydrocephalus. Childs Nerv Syst 2011;27:1595-1608.

78. Corte AD, de Souza CFM, Anes M, et al. Correlation of CSF flow using phase-contrast MRI with ventriculomegaly and CSF opening pressure in mucopolysaccharidoses. Fluids Barriers CNS 2017;14:23.

79. Lalou AD, Levrini V, Czosnyka M, et al. Cerebrospinal fluid dynamics in non-acute post-traumatic ventriculomegaly. Fluids Barriers CNS 2020;17:24.

80. Kapsalaki E, Svolos P, Tsougos I, Theodorou K, Fezoulidis I, Fountas KN. Quantification of normal CSF flow through the aqueduct using PC-cine MRI at 3T. Acta Neurochir Suppl 2012;113:39-42.

81. Wenz F, Hess T, Knopp MV, et al. 3D MPRAGE evaluation of lesions in the posterior cranial fossa. Magn Reson Imaging 1994;12:553-558.

82. Saranathan M, Tourdias T, Kerr AB, et al. Optimization of magnetization-prepared 3-dimensional fluid attenuated inversion recovery imaging for lesion detection at 7 T. Invest Radiol 2014;49:290-298.

83. Gramsch C, Nensa F, Kastrup O, et al. Diagnostic value of 3D fluid attenuated inversion recovery sequence in multiple sclerosis. Acta Radiol 2015;56:622-627.